Clim Dyn (2011) 36:1155–1171
DOI 10.1007/s00382-010-0763-9

The impact of atmospheric initialisation on seasonal prediction of tropical Pacific SST

Debra Hudson · Oscar Alves · Harry H. Hendon · Guomin Wang

Received: 3 August 2009 / Accepted: 8 February 2010 / Published online: 25 February 2010

Abstract The impact of realistic atmospheric initialisation on the seasonal prediction of tropical Pacific sea surface temperatures is explored with the Predictive Ocean–Atmosphere Model for Australia (POAMA) dynamical seasonal forecast system. Previous versions of POAMA used data from an Atmospheric Model Intercomparison Project (AMIP)-style simulation to initialise the atmosphere for the hindcast simulations. The initial conditions for the hindcasts did not, therefore, capture the true intra-seasonal atmospheric state. The most recent version of POAMA has a new Atmosphere and Land Initialisation scheme (ALI), which captures the observed intra-seasonal atmospheric state. We present the ALI scheme and then compare the forecast skill of two hindcast datasets, one with AMIP-type initialisation and one with realistic initial conditions from ALI, focussing on the prediction of El Niño. For eastern Pacific (Niño3) sea surface temperature anomalies (SSTAs), both experiments beat persistence and have useful SSTA prediction skill (anomaly correlations above 0.6) at all lead times (forecasts are 9 months duration). However, the experiment with realistic atmospheric initial conditions from ALI is an improvement over the AMIP-type initialisation experiment out to about 6 months lead time. The improvements in skill are related to improved initial atmospheric anomalies rather than an improved initial mean state (the forecast drift is worse in the ALI hindcast dataset). Since we are dealing with a coupled system, initial atmospheric errors (or differences between experiments) are amplified though coupled processes which can then lead to long lasting errors (or differences).

Keywords Seasonal prediction · Dynamic model initialisation · ENSO prediction · Atmosphere–ocean coupling · Prediction skill · Global coupled ocean–atmosphere modelling

1 Introduction

Prediction of El Niño-Southern Oscillation (ENSO) is generally viewed as an ocean initial condition problem. Skilful prediction of ENSO using coupled ocean–atmosphere climate models of varying degrees of complexity is possible many months in advance without the use of observed atmospheric initial conditions (e.g. Chen et al. 2004; Keenlyside et al. 2005; Luo et al. 2005a; Zhang et al. 2003). Instead of using observed atmospheric initial conditions, some dynamical seasonal prediction systems have generated atmospheric initial conditions from long atmosphere-only model integrations forced with observed sea-surface temperatures (SSTs), such as Atmospheric Model Intercomparison Project (AMIP)-type experiments (e.g. the National Centers for Environmental Prediction's (NCEP) first generation dynamical seasonal prediction system, Ji et al. 1998). The atmospheric initial conditions produced by these AMIP integrations contain low-frequency atmospheric information that is related to anomalous SST in a consistent fashion, but they do not capture the true atmospheric state, especially that associated with tropical intra-seasonal variability that is known to strongly interact with the tropical oceans (e.g. Kessler and Kleeman 2000; Bergman et al. 2001; Zhang et al. 2001; Hendon et al. 2007; Shi et al. 2009).

D. Hudson (✉) · O. Alves · H. H. Hendon · G. Wang
Centre for Australian Weather and Climate Research (CAWCR), A partnership between the Australian Bureau of Meteorology and CSIRO, Bureau of Meteorology, GPO Box 1289, Melbourne, VIC 3001, Australia
e-mail: D.Hudson@bom.gov.au

It would seem to be obvious that there is some benefit from using observed atmospheric initial conditions for dynamical seasonal prediction. However, there has been limited study of its benefit, especially in a coupled model context. For instance, Reichler and Roads (1999) concluded that atmospheric initial conditions can be important for seasonal forecasting, particularly where boundary forcing is weak. They found that with the same boundary forcing, realistic initial conditions resulted in improved forecasts compared to AMIP-type initial conditions out to 5–6 weeks. Phelps et al. (2004) arrived at a slightly different conclusion in a potential predictability study. They found that atmospheric initial conditions had very little impact on prediction for lead times of 1 month or greater. In contrast, Anderson and Ploshay (2000) found large and long-lasting differences (out to the full 3.5 months lead time examined) between a forecast ensemble initialised with AMIP-type initial conditions and an ensemble with observed (NCEP reanalysis) atmospheric initial conditions. However, the latter caution that long-term effects of model spin-up or initialisation shock may occur when using observed initial conditions. Importantly, the predictability studies mentioned above all used uncoupled atmospheric GCMs forced by observed SSTs rather than using coupled models that predict SST. They focused on the predictability signal from the low-frequency component of the atmospheric initial conditions but they did not consider possible coupled-feedbacks between the atmospheric initial conditions and the ocean.

Most operational centres performing coupled model seasonal prediction do use analysed atmospheric observations for their atmospheric initial conditions (e.g. NCEP's second generation prediction system, Kanamitsu et al. 2002; European Centre for Medium Range Weather Forecasts (ECMWF) seasonal forecast system, Stockdale et al. 1998). As mentioned earlier, there are alternative methods of initialisation (e.g. Luo et al. 2005a) that also produce skilful seasonal forecasts without assimilating atmospheric observations into the initial condition. In the latter, the atmospheric initial condition is in balance with the atmospheric model and initialisation shock is reduced, although it has not been proven that this necessarily results in more skilful forecasts. A recent study examining the impact of ocean initialisation on seasonal forecast skill concluded that the most skilful scheme is that which makes the most use of the observed data, even though initial imbalances in the coupled state are generated (Balmaseda and Anderson 2009). However, similar such studies for the benefit of atmospheric initialisation are lacking.

The aims of this paper are twofold. Firstly, we present a new Atmosphere Land Initialisation (ALI) Scheme for the Predictive Ocean–Atmosphere Model for Australia (POAMA), the dynamical seasonal forecast system that is run operationally at the Australian Bureau of Meteorology (BoM). Secondly, we assess the impact of using these realistic atmosphere/land initial conditions from ALI on SST basic-state drift and seasonal forecast skill in the Pacific region, especially that associated with ENSO. In particular, we investigate the influence of the atmospheric initial conditions on the coupled system as a whole, where feedback between the atmosphere and ocean can occur. Although many studies have assessed the role of stochastic intra-seasonal atmospheric variability (especially the Madden–Julian Oscillation; MJO) for ENSO prediction and evolution (e.g. Kessler and Kleeman 2000; Bergman et al. 2001; Zhang et al. 2001; Hendon et al. 2007), and in particular for the development of the 1997/98 El Niño event (e.g. van Oldenborgh 2000; Boulanger et al. 2001; Vitart et al. 2003; Shi et al. 2009), there has not been a comprehensive, controlled assessment of the impact of atmospheric initialization on ENSO seasonal prediction using a coupled forecast model.

POAMA is a coupled ocean/atmosphere model seasonal forecast system, and the first version, POAMA-1 (Alves et al. 2003; Shi et al. 2009), was run operationally by the BoM from 2002 to 2007. When run in real-time, the atmospheric initialisation for the POAMA-1 system came directly from the BoMs' global numerical weather prediction (NWP) forecast system by simply interpolating them onto the POAMA-1 atmospheric model grid. Hindcasts (or retrospective forecasts) from POAMA-1 were generated using atmospheric initial conditions from an AMIP-style atmosphere-only integration of the atmospheric component of POAMA. The land surface of POAMA-1 was initialised to the climatological values produced from an AMIP integration for both the hindcasts and real-time forecasts. This is a common means of initialising the land surface for seasonal prediction. For example, five of the seven coupled atmosphere–ocean GCMs participating in the Climate Prediction and its Application to Society (CliPAS) project used climatological land surface conditions as the initial condition, while two were initialized to the land surface conditions from the NCEP reanalyses (Wang et al. 2009).

The new ALI scheme involves the creation of a new atmosphere/land-surface analysis using the atmospheric model of POAMA. This dataset is then used for the initial conditions of the hindcasts and forecasts. The scheme generates realistic atmospheric initial conditions, as well as land surface initial conditions that are in balance with this atmospheric forcing. The ALI scheme was incorporated into the operational system, POAMA1.5, in January 2008.

Section 2 provides a brief description of the POAMA1.5 forecast system and the hindcast datasets. Section 3 describes ALI and briefly assesses the new ALI analysis dataset compared to the AMIP dataset used previously for

initialisation. Section 4 examines the impact of the ALI initial conditions on forecast skill and drift at seasonal time scales over the Pacific and Sect. 5 describes two case studies. Section 6 provides a general summary and conclusion.

2 POAMA model, hindcast datasets and verification method

The atmospheric model component of POAMA is the BoM's atmospheric model (BAM version 3.0; Colman et al. 2005; Wang et al. 2005; Zhong et al. 2006) which has a T47 horizontal resolution and 17 levels in the vertical. The land surface component of BAM 3.0 is a simple bucket model for soil moisture (Manabe and Holloway 1975) and has three soil levels for temperature. The ocean model is the Australian Community Ocean Model version 2 (ACOM2) (Schiller et al. 1997, 2002), and is based on the Geophysical Fluid Dynamics Laboratory Modular Ocean Model (MOM version 2). The ocean grid resolution is 2° in the zonal direction and in the meridional direction it is 0.5° at the equator and gradually increases to 1.5° near the poles. The atmosphere and ocean models are coupled using the Ocean Atmosphere Sea Ice Soil (OASIS) coupling software (Valcke et al. 2000).

This study uses version 1.5 of POAMA that has improvements over POAMA-1 including a re-tuning of the ocean vertical mixing to reduce excessive noise in east Pacific SSTs, an increase in the coupling frequency (3 h compared to 1 day) in order to resolve the diurnal cycle in some coupled processes, and the inclusion of stress/current coupling i.e. the wind-stress provided from the atmospheric model to the ocean model takes into account ocean surface currents following Luo et al. (2005b). Two versions of POAMA-1.5 are assessed: POAMA-AMIP which uses the AMIP-style integration of BAM to initialise the atmospheric model for the hindcasts (as was done for POAMA-1) and POAMA-ALI which uses the ALI Scheme. The AMIP-style integration used to initialise POAMA-AMIP is an atmosphere-only (BAM) simulation from 1980 to 2001 forced with observed SSTs. Weekly analyses of Reynolds et al. (2002) are used for the period December 1981–2001 and the HadISST monthly analyses (Rayner et al. 2003) are used for January 1980–November 1981.

In order to assess the skill of a seasonal forecasting system and calibrate model errors, it is necessary to conduct a number of retrospective forecasts or hindcasts. Our hindcast datasets have forecasts of 9 months duration, starting on the first day of every month. Here we define a lead time of 1 month as the mean of first month of the forecast. For this study, two hindcast datasets are assessed:

1. POAMA-AMIP: a three member ensemble extending from 1980 to 2001, where the forecasts have AMIP atmosphere and land initial conditions.
2. POAMA-ALI: a ten member ensemble extending from 1980 to 2006, where the forecasts have ALI atmosphere and land initial conditions.

The ocean initial conditions in the POAMA-AMIP and POAMA-ALI experiments are identical and are obtained from the ocean data assimilation scheme that is based on the optimum interpolation (OI) technique of Smith et al. (1991). Only temperature observations in the top 500 m are assimilated and SST is strongly relaxed to the observed analysis (Reynolds et al. 2002). The OI scheme is used to correct the ocean model background field every 3 days using a 3-day observation window. Corrections to ocean currents are calculated by applying the geostropic relation to the temperature increments, similar to the method described by Burgers et al. (2002).

The ten-member POAMA-ALI ensemble is generated through perturbing the atmospheric initial conditions by successively initialising each member with the atmospheric analysis 6 h earlier (i.e. the tenth member was initialised 2.25 days earlier than the first member). The three-member POAMA-AMIP ensemble is generated by initialising with the atmospheric analysis 1 day earlier (i.e. the third member was initialised 2 days earlier than the first member). There is no perturbation applied to the ocean initial conditions.

In Sect. 4 we compare the skill of the POAMA-AMIP and POAMA-ALI systems over the common period of 1980–2001 to assess the impact of the atmosphere-land initialisation. Skill is assessed using forecast anomalies. These are created by producing a lead-time dependent ensemble mean climatology from the hindcasts. Forecasts are compared against this climatology to create anomalies, and in so doing a first-order linear correction for model bias or drift is made (similar to the method of Stockdale 1997). POAMA-ALI has more ensemble members than POAMA-AMIP, thus uncertainty due to initial conditions is better represented in POAMA-ALI, potentially giving improved forecasts solely due to having more ensemble members. Hence, to more fairly compare the intrinsic skill of the two systems, we have used a three-member ensemble mean from POAMA-ALI for assessing the impact of atmosphere/land initialisation on forecast skill and drift. The SST verification data are the Reynolds OI.v2 Sea Surface Temperatures (Reynolds et al. 2002) from December 1981 onwards and prior to this they are from HadISST (Rayner et al. 2003).

3 ALI: atmosphere–land initialisation scheme

ALI uses a nudging scheme in a forecast-analysis cycle to produce the atmospheric and land surface initial conditions

for the hindcasts and real-time seasonal forecasts. A similar method has been used by the Climate Change Prediction Program (CCPP) and Atmospheric Radiation Measurement (ARM) Program in the CCPP-ARM Parametrization Testbed to provide initial conditions for the evaluation of climate models in NWP-mode (Phillips et al. 2004). For ALI, an offline version of the POAMA atmospheric model, BAM, is nudged towards "reality", which we take to be the analyses from ERA-40 (Uppala et al. 2005) for the period 1980 to August 2002, and to be the BoMs' operational global NWP analysis thereafter. ERA-40 has been chosen as the analysis for the hindcasts because the operational global NWP system at the BoM does not have continuous analyses back to 1980.

During the forecast-analysis cycle of ALI, a 6-h atmosphere-only forecast with BAM is made. BAM is forced with observed daily SST, interpolated from the weekly analyses of Reynolds et al. (2002). After completion of the 6-h forecast, the forecast fields of horizontal wind, temperature and humidity are adjusted by addition of the fractional difference with the observed analysis. The fractional difference is controlled by the nudging factor that can vary between 0 (no adjustment) and 1 (completely replace the forecast with the observed analysis). This forecast-analysis cycle is shown schematically in Fig. 1. The adjusted forecast is used as the initial conditions for the next 6-h forecast cycle. At the start of this next forecast cycle, the "adjusted" analysis is filtered by projection onto the model's normal modes (Seaman et al. 1995), which avoids excitation of spurious gravity waves at the initial time of the forecast. The data at the end of each 6-h forecast (prior to adjustment) is output and is used as initial conditions for the hindcasts and forecasts of the POAMA seasonal forecast system.

In the ALI forecast-analysis cycle, the land surface is initialised indirectly via the nudged atmosphere, such that the soil moisture and temperatures evolve to become consistent with the atmospheric forcing. This approach of initialising the land surface does not attempt to correct biases in the land surface model, but it may offer improvements over using climatological land initial conditions. A better way to initialise the land surface might be to force an offline version of the land surface model with observed meteorological forcing. However, this is not an option for the current POAMA system as the land surface model cannot be uncoupled from the atmospheric model.

Consistency between the real-time seasonal forecasts and the hindcasts is important because the hindcasts are used to comprehensively assess the skill of the real-time forecasts and they are used to remove model drift and systematic biases (through the creation of anomalies using a lead-time dependant model climatology). The POAMA-1 system lacked consistency in that the hindcasts were initialised close to the atmospheric model's attractor (because they used an AMIP-type simulation for atmospheric initial conditions) and the real-time forecasts were initialised close to the "real-world" attractor (because they used global analyses from the BoM NWP system for initial conditions). If we chose to use ERA-40 directly in the hindcasts, then we would be initialising the model close to the "real-world" attractor. However, because the initial conditions would then be generated from a different model to BAM, there would be initial shock to the system, which can cause degradation of forecast skill, particularly if there are serious model errors. In addition, consistency between the hindcasts and real-time forecasts would be reduced. In other words, the stronger the nudging (the higher the nudging coefficient), the greater the dependency on the

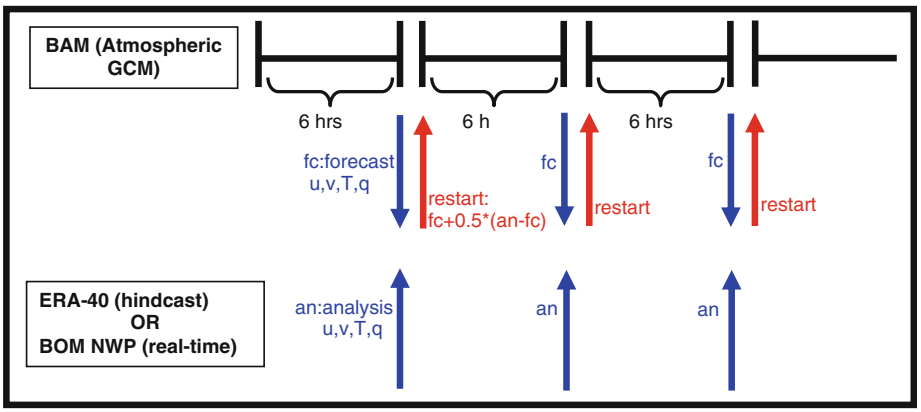

Fig. 1 Schematic of the atmosphere–land initialisation scheme (ALI). Every 6 h the BoMs' atmospheric model (BAM) is stopped and its forecast (fc) of u-wind, v-wind, temperature (T) and humidity (q) at all levels is compared to an analysis (an) (ERA-40 for the hindcasts or the BoM numerical weather prediction analysis for real-time). Half the difference between the forecast and the analysis is added to the BAM forecast and the model is restarted and allowed to freely evolve for the next 6 h. This is done repeatedly, thus nudging BAM towards the analysis at each step

source of initial conditions (e.g. ERA-40 or the NWP system) and, potentially, the bigger the shock. After initial experimentation we chose to nudge BAM halfway towards the analysis (nudging coefficient of 0.5). For the hindcasts this means that more realistic (closer to the "real-world" attractor) atmosphere and land initial conditions are incorporated compared to the POAMA-1 system and there is reduced shock to the system compared to using ERA-40 initial conditions directly. For the real-time forecasts, this nudging reduces sensitivity to inevitable changes in the analyses from the operational NWP system (such as changes to resolution and model physics), and it acts as a buffer that improves consistency with the hindcasts. Furthermore, the same land surface model is used for the initialisation phase and the forecast phase. This reduces problems associated with a different land surface model being used by the operational NWP system and the POAMA system that is run in real-time.

Essentially the ALI system offers a compromise between initialising the model close to the real-world attractor and the model attractor. It also reduces dependency on the model used to generate the initial conditions and in so doing improves consistency between the hindcasts and forecasts.

The output from the ALI forecast-analysis cycle is called the BAM-ALI analysis and this new analysis is used as initial conditions for the hindcasts and forecasts. We compare BAM-ALI, used to initialise the POAMA-ALI experiment, with the AMIP initial conditions (hereafter referred to as BAM-AMIP), used to initialise the hindcast dataset of POAMA-1 and the POAMA-AMIP experiment. As expected, the BAM-AMIP initial conditions capture much of the low frequency atmospheric variability driven by slow variations of SST (e.g. the seasonal mean westerly anomalies in the equatorial western Pacific during El Niño years). However, even these slow variations are better depicted in the BAM-ALI initial conditions. Figure 2 shows the time series of differences in monthly u-wind anomalies at 10 m (u10) (climatological seasonal cycle of the datasets has been removed) area-averaged over the western Pacific for BAM-ALI and BAM-AMIP with respect to ERA-40. The interannual anomalies from BAM-ALI are much closer than BAM-AMIP in magnitude and temporal behaviour to ERA-40 (the correlation of each time series with ERA-40 is 0.99 and 0.59, respectively). Furthermore, the BAM-AMIP initial conditions are unable to capture observed intra-seasonal variability, as depicted in the ERA-40 reanalysis, whereas the BAM-ALI initial conditions can. For example, Fig. 3 shows a longitude-time plot for January to March 1985 for outgoing longwave radiation (OLR) (averaged between 20°S and 20°N), a variable that is not nudged to ERA-40. The coherent eastward propagation of convection associated with the MJO in February 1985 is largely reproduced by BAM-ALI, but, as to be expected, is not by BAM-AMIP. This better agreement of BAM-ALI to ERA-40 is also reflected by the reduction of the bias in the BAM-ALI initial conditions. For example, Fig. 4 shows the January climatological (1980–2002) bias from BAM-ALI and from BAM-AMIP with respect to ERA-40 for u10. It is clear that the nudging process has reduced the biases, for example as seen in the reductions of the strong westerly bias over the western Pacific, the easterly bias over the Indian Ocean, and the more modest easterly bias over the central-eastern Pacific.

A comprehensive comparison of the BAM-ALI and BAM-AMIP initial conditions is beyond the scope of this paper, but suffice to say that the nudging process to create BAM-ALI works well and produces more realistic initial conditions than BAM-AMIP.

4 Impact of ALI on seasonal prediction

4.1 Forecast skill

In this section we examine the impact of the improved atmospheric initial conditions on the skill of the seasonal forecasts. We expect increased skill at intra-seasonal timescales from using BAM-ALI initial conditions, but it is not necessarily obvious that more realistic atmosphere/land initial conditions would make a difference at the seasonal scale, particularly for predictions of tropical Pacific SST. Figure 5a shows the Niño3 SST anomaly correlation for all start months for POAMA-AMIP and POAMA-ALI. We also compare with persisted SST anomalies (persisting the observed monthly mean SSTA from the month immediately

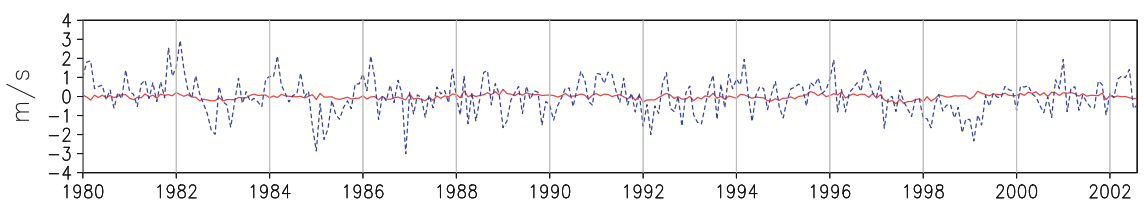

Fig. 2 Timeseries of differences in monthly u10 (m s^{-1}) area-averaged over the western Pacific (10°S–10°N, 120°E–180°E) for BAM-ALI minus ERA-40 (*red solid line*), and BAM-AMIP minus ERA-40 (*blue dashed line*)

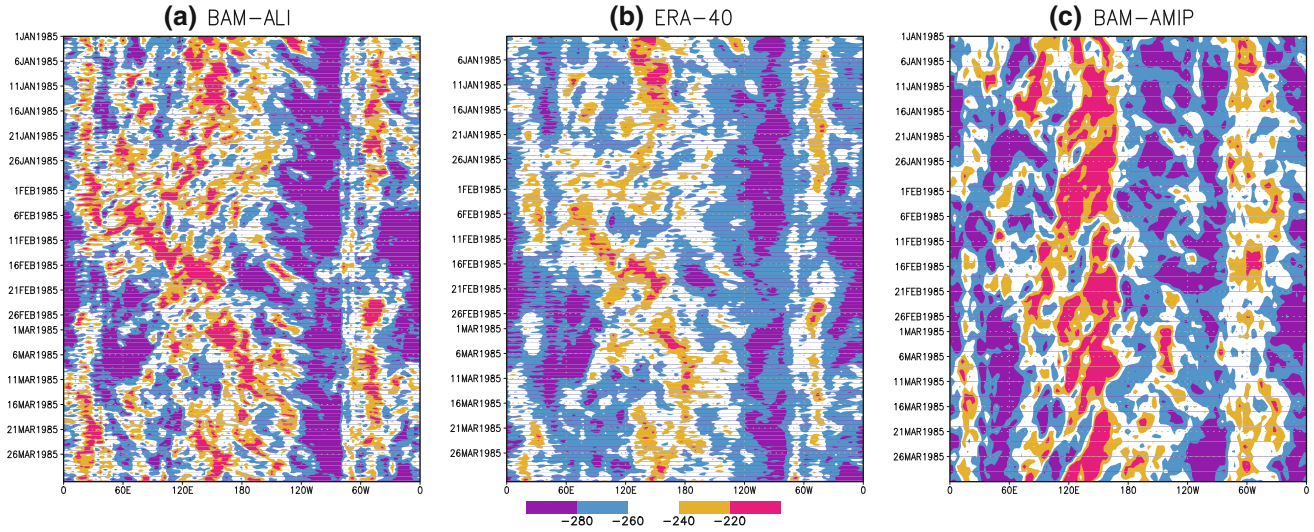

Fig. 3 Longitude-time plot for January–March 1985 of OLR (W m^{-2}) (averaged between 20°S and 20°N) from **a** BAM-ALI (6-h data shown), **b** ERA-40 reanalysis (6-h data shown), and **c** BAM-AMIP (daily data shown, since the 6-h output was not available)

Fig. 4 January long-term average (1980–2002) u10 bias (m s^{-1}) over the equatorial Indian and Pacific Oceans for **a** BAM-ALI and **b** BAM-AMIP, with respect to the ERA-40 reanalysis. Contour interval is 1 m s^{-1}

prior to the forecast start date). Both POAMA-AMIP and POAMA-ALI beat persistence and have a correlation above 0.6 at all lead times. POAMA-ALI, which uses ALI initial conditions, is an improvement over POAMA-AMIP out to about 6 months lead time. A similar result is obtained with mean-square error (MSE), for which statistically significant reductions in MSE are obtained to 6 months lead (details in Fig. 5b). In general, POAMA-ALI shows a skill improvement of about 1 month lead over POAMA-AMIP (e.g. POAMA-ALI achieves a correlation skill above 0.8 out to 5 months lead, whereas POAMA-AMIP achieves it only out to 4 months lead). Results over the central Pacific (Niño34) are much the same, with significant improvement in POAMA-ALI over POAMA-AMIP evident out to 6 months lead time for MSE (not shown).

In summary, improving the atmosphere and land initial conditions improves the skill of forecasting central and eastern equatorial Pacific SSTs out to about 6 months lead time. This skill improvement does, however, vary depending on the time of year. Most of the improvement is found for start months in the austral winter (JJA) and spring (SON) (Fig. 6). We do not know why there is this seasonal difference in the improvement of skill, and this question is still under investigation. It may be related to the typical ENSO life cycle and the possible role of the MJO. Forecasts starting in the June to November months are associated with the onset of El Niño events, and the westerly wind anomalies associated with the MJO, which can project onto the developing coupled El Niño mode (e.g. Hendon et al. 2007), are better depicted in POAMA-ALI than in POAMA-AMIP.

In order to understand how the difference in atmospheric initial conditions between ALI and AMIP impacts the predicted Niño3 SSTA, we correlate the difference between the predicted Niño3 SSTA from POAMA-ALI and POAMA-AMIP at a lead time of 3 months with the difference in surface wind (u10) anomalies (averaged between 5°S and 5°N) from the POAMA-ALI and POAMA-AMIP forecasts starting from the initial time. For this analysis, we have grouped the winter and spring (JJASON) and summer and autumn (DJFMAM) forecast start months together. As expected, differences in Niño3 at 3 months lead are associated with differences in zonal wind anomalies over the central equatorial Pacific for both seasons (Fig. 7). For start months in DJFMAM, differences in the prediction of Niño3 cannot, however, be clearly traced back to differences in the equatorial surface wind in the initial conditions (Fig. 7a), although they may be related to other differences at the initial time. In contrast, in JJASON the difference in the Niño3 prediction can be traced back to differences in surface wind initial conditions over the western Pacific (120°–180°E) (Fig. 7b). Spatial

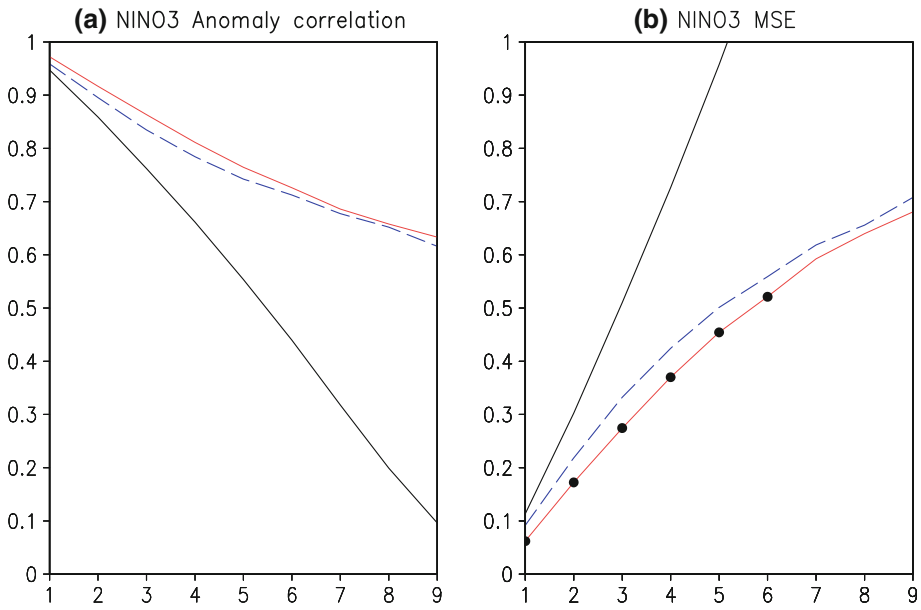

Fig. 5 Niño3 sea-surface temperature **a** anomaly correlation skill and **b** mean-square error (MSE) (°C) as a function of lead time (months, *x*-axis) for all forecast start months. The *black solid line* is for persistence, the *blue dashed line* for the POAMA-AMIP ensemble mean and the *red solid line* for the POAMA-ALI ensemble mean. Calculations are performed with ensemble means calculated from three hindcast members for both POAMA-ALI and POAMA-AMIP. The *black dots* indicate lead times where the POAMA-ALI MSE is significantly smaller than the POAMA-AMIP MSE (0.10 significance level, one-tailed *t* test, $n = 264$)

plots of the difference in u10 at the initial time with the difference in the Niño3 prediction at 3 months lead (Fig. 8) also show the strong sensitivity to zonal wind differences (and by inference, errors) in the western Pacific at the initial time for JJASON. In JJASON the difference in initial u10 anomalies (as related to the difference in predicted Niño3 SSTA) appears to propagate eastward into the central Pacific in the first month of the forecast and is then maintained around the dateline for the subsequent 2 months (Figs. 7b, 8b). Essentially, the initial equatorial wind field in JJASON, particularly over the western Pacific, is important in determining what happens to SSTAs in subsequent months. Presumably, zonal wind anomalies in the western Pacific are more realistically depicted in ALI, hence POAMA-ALI is more skilful than POAMA-AMIP. More realistic wind initial conditions in POAMA-ALI result in improved wind (u10) skill over the tropical oceans in the first month of the forecast (Fig. 9). More realistic wind anomalies in the first month in POAMA-ALI are translated into improved SST anomaly predictions at longer lead times. That is, errors in the AMIP initial conditions are translated into erroneous low frequency SST anomalies via a coupled response.

4.2 Forecast drift

The analysis thus far has assessed the impact of atmospheric initial conditions on forecast skill after removal of the model's mean bias or drift. Model bias was removed through the creation of anomalies using a lead-time dependant model climatology for POAMA-AMIP and POAMA-ALI, respectively. This approach facilitates the analysis of the intra-seasonal and seasonal signals even in the presence of large drift. However, an appropriate question to ask is whether prediction skill is improved over the Pacific in POAMA-ALI compared to POAMA-AMIP due to better simulation of the mean state or better initialisation of the anomalies? In other words, has improved initial conditions provided by ALI led to reduced mean state bias and hence improved predictions?

Figure 10a–c show longitude/forecast lead-time plots for all forecast start months of the POAMA-AMIP SST bias, as well as the mean difference between POAMA-ALI and POAMA-AMIP for both SST and u10 (a 7-day running mean has been applied to the u10 daily data). The POAMA-AMIP model drifts towards colder SSTs over the duration of the 9 month forecast, reaching a 2°C cold bias for the last couple of months over much of the equatorial Pacific (Fig. 10a). An exception is over the far eastern Pacific, which tends to have a warm bias. The cause of the mean bias in POAMA-AMIP, especially the cold SST bias throughout much of the tropics, is not addressed here, but it stems from atmospheric model error (e.g. too much cloud and too strong latent heat flux over the western and central Pacific). Here we concentrate on the relative differences between POAMA-AMIP and POAMA-ALI. Relative to POAMA-AMIP, POAMA-ALI exhibits an easterly wind bias over the far western Pacific for the first 10 days of the forecasts, which then propagates into the central Pacific during the first month of the forecast, where it is maintained for the entire 180 days shown here (Fig. 10c). This leads to POAMA-ALI being relatively colder than POAMA-AMIP in the central Pacific (primarily in the Niño3.4 region) 2–4 months into the forecast, but it is maintained for the full 9 months of the forecast (Fig. 10b). Figure 10a, b can be summarized in the plot of Niño3.4 SST drift for

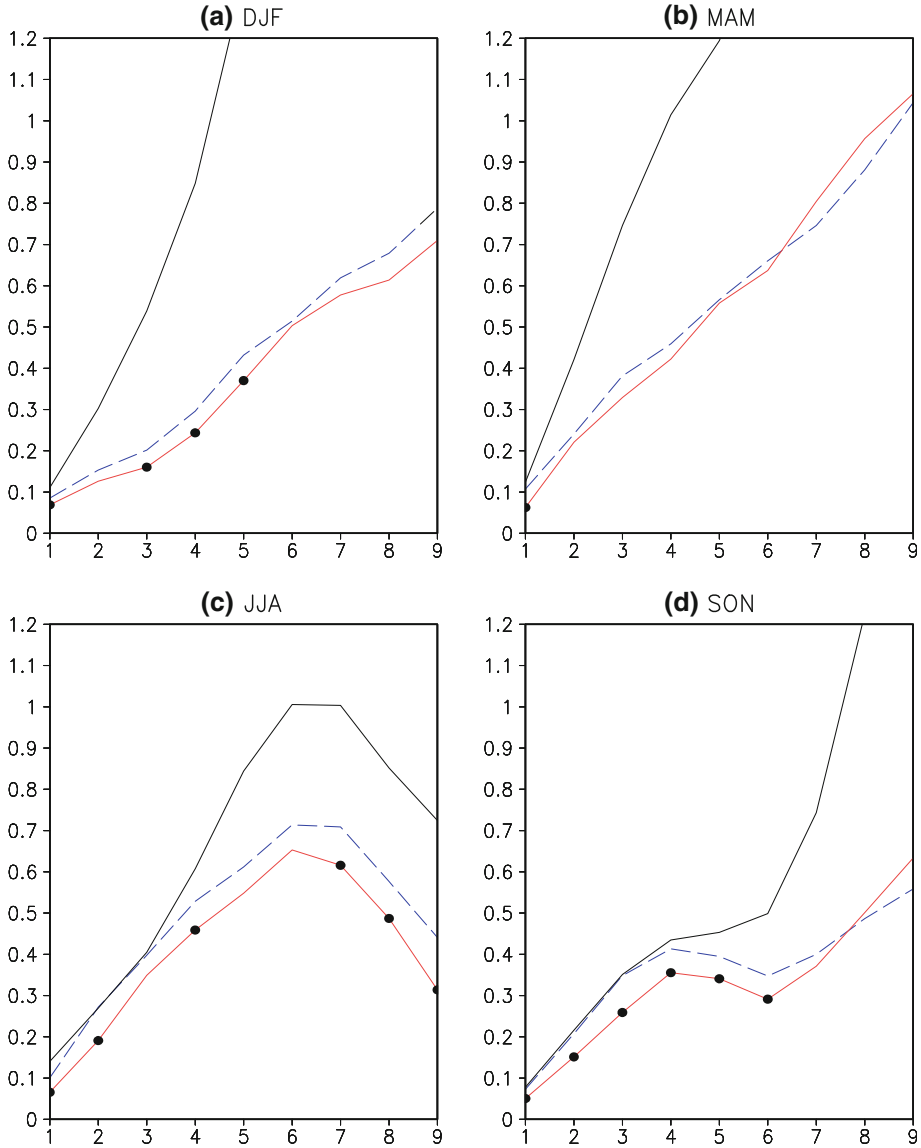

Fig. 6 Niño3 sea-surface temperature MSE (°C) as a function of lead time (months, *x*-axis) for forecast start months **a** December, January and February (DJF), **b** March, April and May (MAM), **c** June, July and August (JJA) and **d** September, October and November (SON). The *black solid line* is for persistence, the *blue dashed line* for the POAMA-AMIP ensemble mean and the *solid red line* for the POAMA-ALI ensemble mean. Calculations are performed with ensemble means calculated from three hindcast members for both POAMA-ALI and POAMA-AMIP. The *black dots* indicate lead times where the POAMA-ALI MSE is significantly smaller than the POAMA-AMIP MSE (0.10 significance level, one-tailed *t* test, $n = 66$)

POAMA-AMIP and POAMA-ALI, shown in Fig. 10d. The model bias is clearly sensitive to the different initialisation of the two systems. Although both systems still drift in the same sense, the cold bias over the Niño34 region is statistically significantly worse in POAMA-ALI (red line) at all lead times (Fig. 10d). It is clear that the improvements in forecast skill in POAMA-ALI compared to POAMA-AMIP (Fig. 5) do not result from reduced drift or bias in the model. On the contrary, POAMA-ALI experiences slightly more drift than POAMA-AMIP.

The development of a greater Pacific cold tongue bias in POAMA-ALI stems from the atmospheric initial conditions for POAMA-ALI that are different from the model's climate attractor because they are designed to be closer to the real-world attractor. Recall that POAMA-ALI is closer to observed (ERA-40) at the initial time (e.g. Fig. 4). As a consequence, at the start of the forecast in POAMA-ALI there is a rapid adjustment of the model atmosphere towards its preferred climatology. This adjustment initiates a coupled response that affects the mean SST for a number of months into the forecast. It is interesting that changing the climatology of the atmospheric initial conditions can have such a long lasting and relatively large effect on the mean-state of the forecast. But, it is not clear how much initialisation shock is limiting our forecast skill. The results shown in this study suggest that even though the drift is larger in POAMA-ALI, the forecast skill of the Niño indices is higher than with POAMA-AMIP. However, we do know from studies with POAMA-ALI that the SST drift in the model is detrimental to, for instance, the teleconnection of ENSO to Australian rainfall as lead time progresses (Lim et al. 2009).

Reducing initialisation shock is not a trivial undertaking, particularly in the face of large model errors. We have

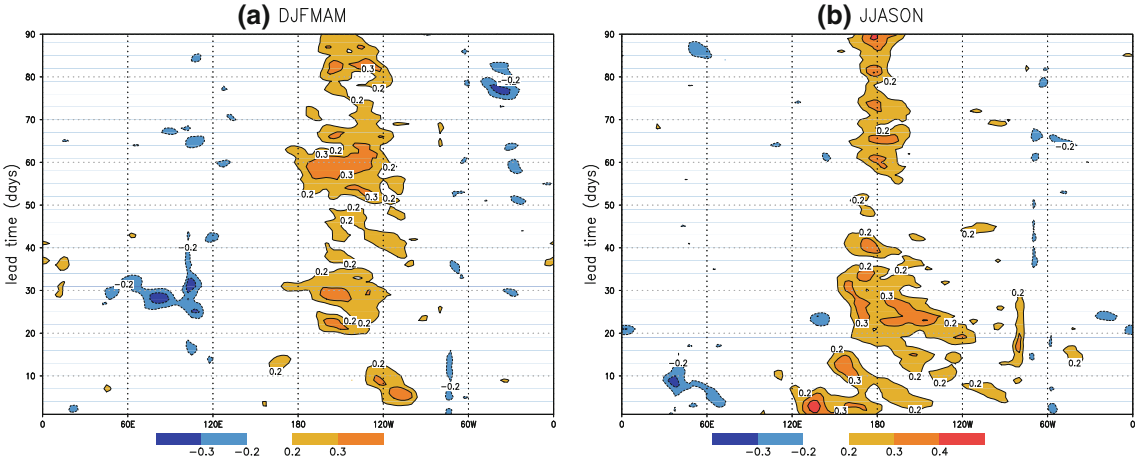

Fig. 7 Longitude-lead time plots of correlations of the difference between the predicted Niño3 SSTA from POAMA-ALI and POAMA-AMIP at a lead time of 3 months (i.e. lead 3: POAMA-ALI Niño3 minus POAMA-AMIP Niño3), with the difference in predicted u10 anomalies (averaged between 5°S and 5°N) from POAMA-ALI and POAMA-AMIP as a function of lead time (days). Data from the 22 years hindcast sets are grouped together for **a** December, January, February, March, April and May (DJFMAM) and **b** June, July, August, September, October and November (JJASON) forecast start months. Significant correlations are shaded (correlations greater than 0.17 are significant at the 0.05 significance level; *t* test, $n = 132$)

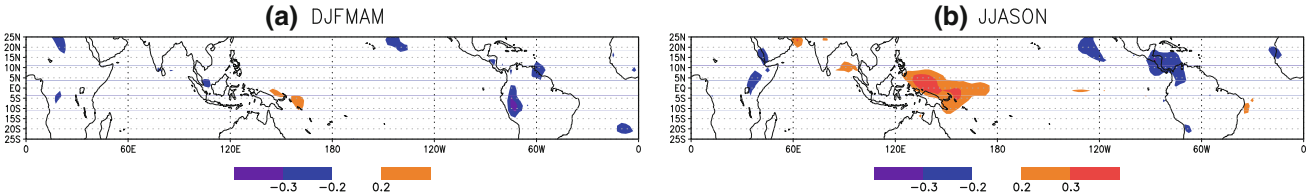

Fig. 8 Correlation of the difference between the predicted Niño3 SSTA from POAMA-ALI and POAMA-AMIP at a lead time of 3 months (i.e. lead 3: POAMA-ALI Niño3 minus POAMA-AMIP Niño3), with the difference in the u10 anomaly initial conditions of POAMA-ALI and POAMA-AMIP (i.e. ALI initial condition minus AMIP initial condition). Data from the 22 years hindcast sets are grouped together for **a** December, January, February, March, April and May (DJFMAM) and **b** June, July, August, September, October and November (JJASON) forecast start months. Significant correlations are shaded (correlations greater than 0.17 are significant at the 0.05 significance level; *t* test, $n = 132$)

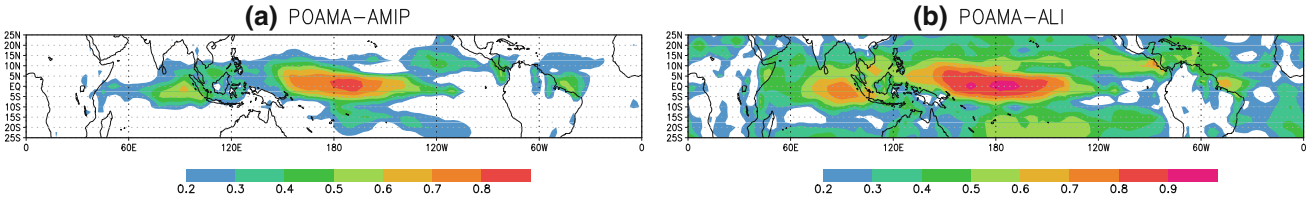

Fig. 9 Monthly mean u10 anomaly correlation with observed after 1 month of the forecast for JJASON forecast start months from **a** POAMA-AMIP and **b** POAMA-ALI. Correlations are performed with ensemble means calculated from three hindcast members for both POAMA-ALI and POAMA-AMIP. Significant correlations are shaded (correlations greater than 0.17 are significant at the 0.05 significance level; *t* test, $n = 132$)

already reduced the initialisation shock by using the ALI scheme (nudging BAM towards ERA-40) rather than initialising with ERA-40 directly. Perhaps we could nudge the ALI analysis less strongly towards ERA-40, thus degrading the initial conditions further, but, based on the outcome of the present study, this would probably come at the cost of reduced forecast skill. Some research centres have addressed this issue by using anomaly initialisation, such that the initial mean state is consistent with the model attractor, but the initial anomalies are consistent with observed anomalies. However, this approach has tended to have little impact on forecast skill (Galanti et al. 2003; Rienecker 2003; Kirtman 2006). The best solution in the long run, of course, is to reduce model biases so that the model can be initialised close to the observed state without generating any shock. A thorough investigation of the

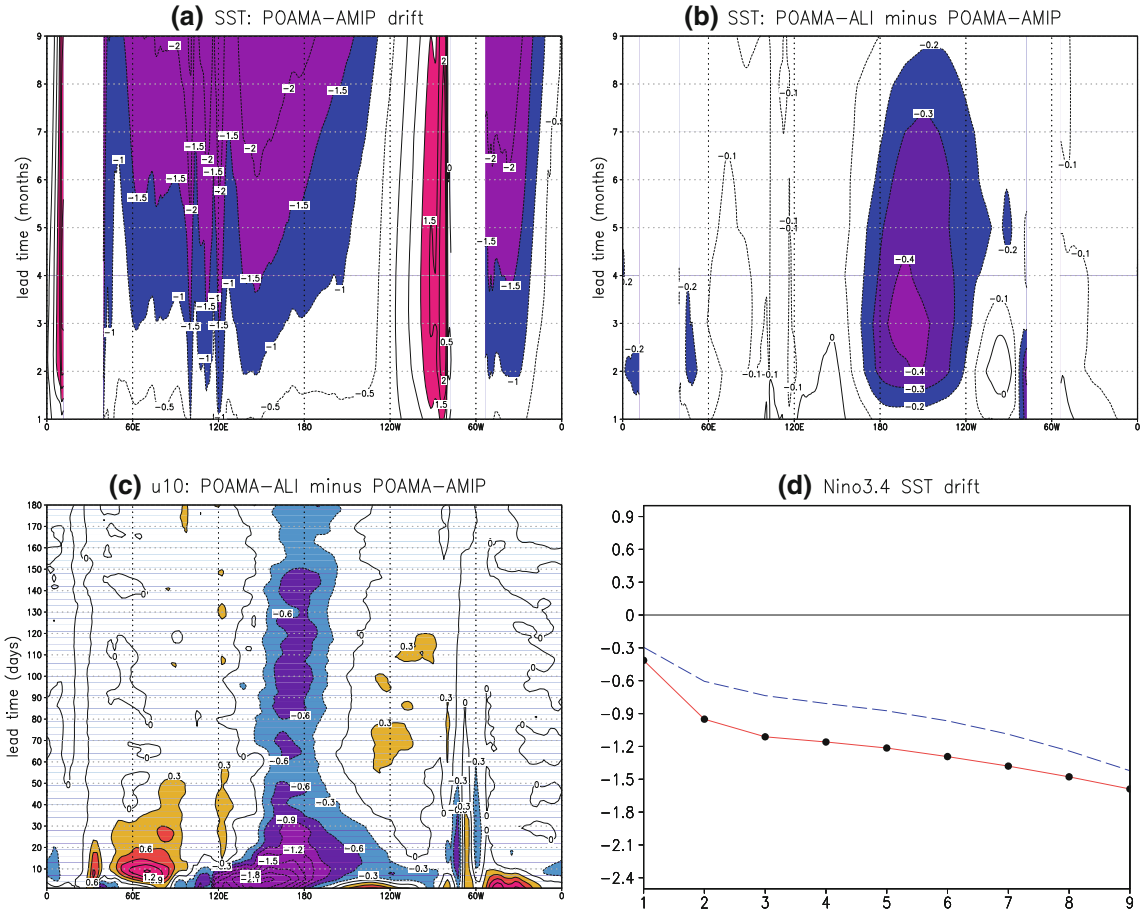

Fig. 10 Longitude-forecast lead time plots (averaged 5°S–5°N) of the **a** SST (°C) drift for POAMA-AMIP with respect to Reynolds OI.v2 SST, **b** climatological mean SST difference between POAMA-AMIP and POAMA-ALI over the 9 month forecast and **c** climatological mean u10 (m s^{-1}) difference between POAMA-AMIP and POAMA-ALI over the first 6 months (daily shown). Plot **d** shows the SST forecast drift (°C) in the Niño3.4 region for POAMA-AMIP (*blue dashed*) and POAMA-ALI (*red solid*) as a function of lead time (months, *x*-axis). The *black dots* indicate lead times where the POAMA-ALI and POAMA-AMIP means are significantly different (0.05 significance level, $n = 264$). Plots are for all forecast start months

impact of initialisation shock is beyond the scope of the current paper, but we can conclude that the increased skill in forecasting equatorial Pacific SST anomalies in POAMA-ALI compared to POAMA-AMIP (Fig. 5) comes from improved initial atmospheric anomalies that better depict variability, rather than from an improved mean state.

4.3 Consistency in initialisation between the hindcast and real-time systems

In a real-time forecasting system, the forecast anomalies are created using the lead-time dependent climatology obtained from the hindcast dataset. The results obtained in the present study emphasize the importance of initialising the atmosphere/land of the hindcast and real-time systems in a consistent manner. We have shown in Sect. 4.2 that the forecast drift, and hence the lead-time dependent climatology, is sensitive to how the atmosphere is initialised. Figure 10d indicates that for all forecast months there is a ~0.4°C difference in the climatologies for lead times 2–4 months over the Niño3.4 region. The standard deviation of Niño3.4 SSTA forecasts over these lead times is 1.03 and 1.05°C for POAMA-ALI and POAMA-AMIP, respectively. So, on average, the difference in the bias correction terms represents about half a standard deviation of the forecast variability. There is, however, seasonal variability in the bias correction terms. For example, for JJA forecast start months the difference in the bias correction terms for lead times 2–4 months for the Niño3.4 region is about 0.7°C. The difference in the bias correction terms (lead-time dependent climatologies) for POAMA-ALI and POAMA-AMIP is thus of a similar magnitude to the forecast signal. This suggests that if the hindcast and real-time forecast systems employ different approaches to atmospheric initialisation (as they did in POAMA-1) the bias correction terms used to calibrate the real-time

forecasts may introduce a significant error into the real-time forecast anomalies. This may also have implications for seasonal forecast systems that use NWP analyses directly for the atmospheric initial conditions, since major changes in the NWP system could lead to different forecast biases in the real-time system. ALI does provide some kind of a buffer to such NWP changes by producing an estimate of the initial state that is more consistent with the GCM performing the seasonal forecast.

5 Case studies

Two case studies have been selected to more clearly demonstrate the translation of erroneous atmospheric initial conditions into sustained spurious SST anomalies via a coupled response. Firstly, we chose the (often studied) onset of the 1997 El Niño. In this example, it will be shown that the observed MJO, or westerly wind burst, in the initial conditions of POAMA-ALI resulted in an improved forecast of the developing El Niño. Secondly, we chose a case (July 1999) where, in contrast to the above case, there was an MJO present in the western Pacific in the initial conditions of POAMA-AMIP, but not in POAMA-ALI (or observed). The consequence of this was that the propagation of the MJO in the POAMA-AMIP forecast caused POAMA-AMIP to warm more over the central and eastern tropical Pacific than POAMA-ALI and observed.

5.1 The 1997 El Niño case study

March 1997 was characterised by strong westerly wind events associated with MJO activity (Fig. 11a). There is evidence that this MJO activity contributed to the rapid development and large amplitude of the 1997/98 El Niño (e.g. McPhaden 1999; van Oldenborgh 2000; Bergman et al. 2001; Boulanger et al. 2001; Lengaigne et al. 2003; Vitart et al. 2003). The POAMA model is able to simulate reasonably realistic MJO events (Zhang et al. 2006; Marshall et al. 2008) and their interaction with El Niño (Shi et al. 2009). Since forecasts from POAMA-ALI have the observed westerly wind events in the initial conditions, POAMA-ALI should be able to capture the timing and intensity of an initial MJO event and its interaction with El Niño better than POAMA-AMIP, thereby leading to an improved forecast of the developing El Niño. Is this the case?

To identify the state of the MJO we use the real-time multivariate MJO (RMM) index (Wheeler and Hendon 2004; Rashid et al. 2010). The RMM is a bivariate index, comprising RMM1 and RMM2 which are calculated by performing a combined EOF analysis of meridionally averaged (15°S–15°N) daily anomalies of the zonal winds at 200 and 850 hPa and OLR. RMM1 and RMM2 are the principal component time series of the resulting leading pair of EOFs. Projection of the observed fields onto the RMM indices follows Wheeler and Hendon (2004), while the projection of the forecast fields onto the RMM index follows the procedure of Rashid et al. (2010). The MJO phase diagram (Wheeler and Hendon 2004) shown in Fig. 11b is a plot of the predicted and observed RMM indices. On the diagram, anticlockwise movement around the origin is indicative of the eastward propagation of the MJO and the amplitude of the MJO is given by the distance from the origin (MJO's falling within the central circle are considered weak). The observed MJO on the 1 March 1997 had its westerly/convective centre in the western Pacific and then propagated systematically into the central Pacific, where sustained westerly anomalies then developed. The forecasts from POAMA-ALI show that this eastward propagation of the MJO is well captured in the first month of the forecasts (Fig. 11b). On the other hand, the MJO rapidly collapses in the POAMA-AMIP forecasts (Fig. 11b), despite the fact that by chance the AMIP initial condition appears to have an MJO of about the right magnitude and phase in the initial condition (further examination of the AMIP initial conditions for surrounding months indicates that the MJO in the AMIP initial conditions indeed has random phase and amplitude compared to the observed MJO). The impact on the prediction of El Niño is demonstrated in Fig. 11c, which shows the observed and 9 month forecast plumes for a start date of 1 March 1997 for Niño3.4 SST anomalies. The POAMA model significantly underestimates the magnitude of the developing El Niño for both cases (most numerical models underestimated the intensity of this El Niño, Vitart et al. 2003), but POAMA-ALI shows an improvement over POAMA-AMIP from months 3–9 (this is also the case for the Niño3 and Niño4 regions).

The link between the westerly wind burst associated with the MJO and the amplitude of the predicted SST anomaly is examined in more detail in Fig. 12, which shows longitude/lead-time plots of POAMA-ALI and POAMA-AMIP u10 anomalies (averaged 5°S–5°N) starting on the 1 March 1997. Differences between the POAMA-ALI and POAMA-AMIP ensemble mean forecast anomalies for u10, the depth of the 20°C isotherm along the equator (Z20) and SST are also shown. The daily data have been smoothed with a 7-day running mean. More pronounced eastward-propagation of the MJO is evident in POAMA-ALI compared to POAMA-AMIP (i.e. anomalous westerlies starting in the western Pacific and propagating eastward across the basin in the first 2 months of the forecast; Fig. 12a, b, c). These anomalous westerlies cause the eastward advection of warmer water on the edge of the warm pool near the dateline, resulting in positive SST

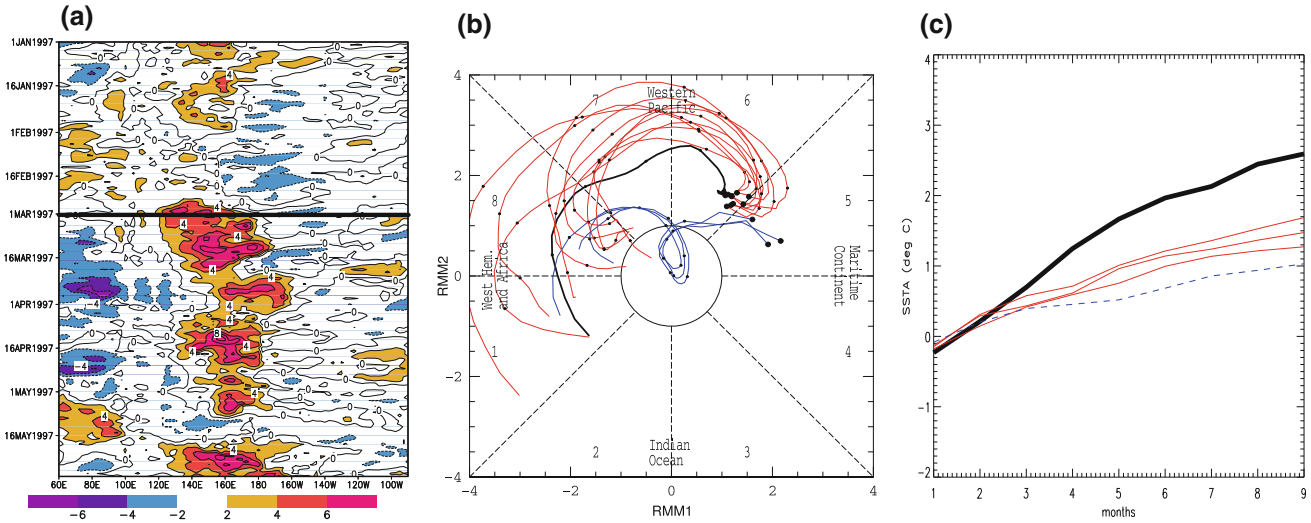

Fig. 11 March 1997 case study. **a** Observed (ERA-40) u10 anomalies. Anomalies greater than 2 m s^{-1} are shaded. The *horizontal line* indicates the date 19970301. **b** Phase diagram (Wheeler and Hendon 2004) of MJO propagation for a forecast start date of 19970301 for observed (ERA-40, *black line*), the ten ensemble members of POAMA-ALI (*red lines*) and the three ensemble members of POAMA-AMIP (*blue lines*). 30-day length trajectories are plotted, with the start date position marked by a *large dot* and *small dots* indicating 5-day intervals. **c** Niño3.4 SSTA over the 9 month forecast period, starting 19970301, for observed (Reynolds OI.v2 SST; thick black line), the POAMA-AMIP ensemble mean (*blue dashed line*) and the POAMA-ALI ensemble mean (*red lines* are three independent ensemble means each comprising three members taken from the original ten member ensemble)

anomalies there after about 20 days of the forecast (Fig. 12e). The westerlies also excite a downwelling Kelvin wave (Fig. 12d) that causes sustained SST warming in the eastern Pacific, thereby resulting in persistent westerly anomalies near the dateline some 60 days into the forecast in POAMA-ALI compared to POAMA-AMIP (Fig. 12c, e). This coupling of intraseasonal variability with the onset of El Niño, as depicted by the difference between POAMA-ALI and POAMA-AMIP, is reminiscent of what actually occurred in 1997 (Bergman et al. 2001). Forecasts from POAMA-ALI also appear to generate a second MJO event (starting around day 40 in the western Pacific), which leads to more warming in the central and eastern Pacific compared to POAMA-AMIP in subsequent months. The generation of the second MJO event may have been by chance, but it could also result from the coupled feedback that altered the SST on the edge of the warm pool in such a fashion as to be conducive to the development of the MJO (e.g. Kessler and Kleeman 2000; Hendon et al. 2007).

5.2 July 1999

Figure 13 shows the MJO phase plot and SSTA plumes for forecasts initialised on 1 July 1999. The observed MJO on 1 July 1999 had a very small amplitude and its westerly/convective centre was located in the western hemisphere/Africa sector (Fig. 13a). Both the observed and predicted MJO from POAMA-ALI then propagated across the Indian Ocean with small amplitude for the next 30 days (Fig. 13a). In contrast, POAMA-AMIP had an initial MJO near the maritime continent and it propagated, with increasing amplitude, into the central Pacific Ocean (Fig. 13a). A consequence of this error in POAMA-AMIP initial conditions is warmer SSTAs over the central and eastern Pacific compared to POAMA-ALI from 2 months onwards in the forecast, hence a larger error compared to observed (Fig. 13b).

The lead-time dependent forecast anomalies of u10, z20 and SST for this case are examined in Fig. 14. POAMA-ALI consistently forecasts easterly wind anomalies over the western Pacific and POAMA-AMIP has a similar tendency (Fig. 14a, b). However, the MJO in the initial condition of POAMA-AMIP results in an eastward propagation of zonal wind anomalies across the Pacific causing westerly wind anomalies over the western Pacific about 20 days into the forecast (Fig. 14a). This eastward propagation of the westerly winds is also highlighted in the difference in wind anomalies between POAMA-AMIP and POAMA-ALI (Fig. 14c). These differences cause differences in the thermocline depth after 20 days over the central and eastern Pacific (Fig. 14d), probably due to the excitation of a downwelling Kelvin wave in POAMA-AMIP compared to POAMA-ALI, and thus results in more warming over the middle and eastern Pacific in POAMA-AMIP compared to POAMA-ALI (Fig. 14e). Essentially, the erroneous atmospheric initial conditions in POAMA-AMIP at the start of July 1999 result in the propagation of an MJO across the equatorial Pacific causing warming of

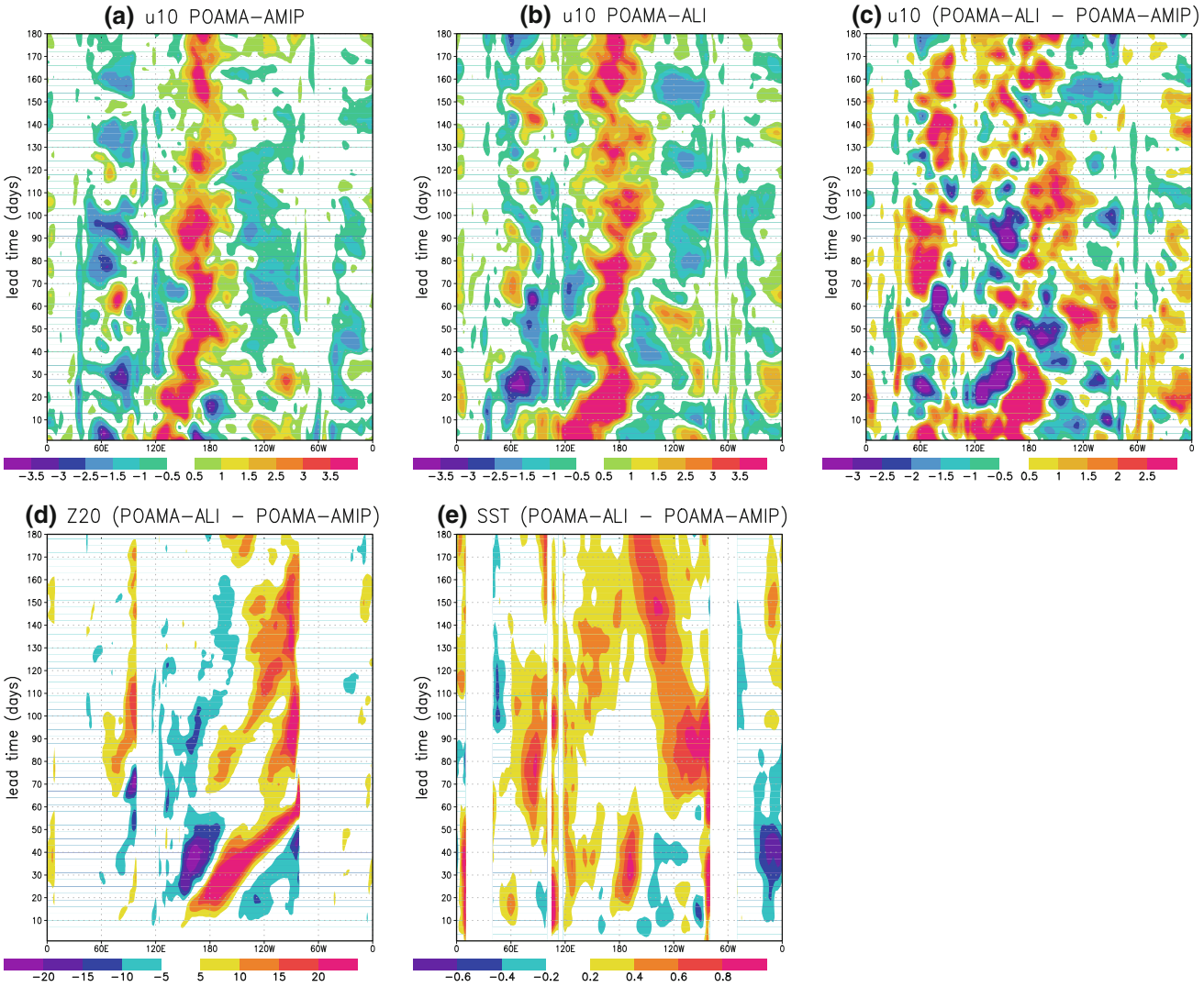

Fig. 12 Longitude-lead time plots for forecasts starting on 1 March 1997 of **a** POAMA-AMIP u10 (m s^{-1}) anomalies averaged between 5°S and 5°N (contour interval 0.5 m s^{-1}), **b** POAMA-ALI u10 (m s^{-1}) anomalies, and POAMA-ALI minus POAMA-AMIP anomalies for **c** u10 (m s^{-1}) (contour interval 0.5 m s^{-1}), **d** depth of the 20°C isotherm (m) along the equator (Z20) (contour interval 5 m) and e) SST (°C) averaged between 5°S and 5°N (contour interval 0.2°C)

SSTAs in the eastern Pacific compared to POAMA-ALI and observed, where no such event occurred.

6 Conclusion

This paper has demonstrated an impact of atmospheric initial conditions on the skill of seasonal forecasts of El Niño using a global coupled model. In particular, more realistic atmospheric initial conditions that better capture the true state of atmospheric intraseasonal variability results in improved seasonal skill for prediction of El Niño at lead times as long as 6 months. Although the atmosphere is typically associated with a short-term memory, atmospheric initial conditions can excite a coupled-response that has a long-lasting impact on the forecast.

We describe an effective nudging method for creating realistic atmospheric initial conditions, called the ALI (atmosphere-land initialisation) scheme. ALI creates initial condition analyses using an offline version of the POAMA atmospheric model and nudging it towards "reality" (ERA-40 for the hindcasts and BoM NWP for the real-time system). ALI has been incorporated into the latest version of the POAMA seasonal forecast system (version 1.5). ALI offers a compromise between initialising close to the model's climate attractor and the real-world attractor. This compromise may be particularly useful when there are reasonably large model biases such that the initialisation

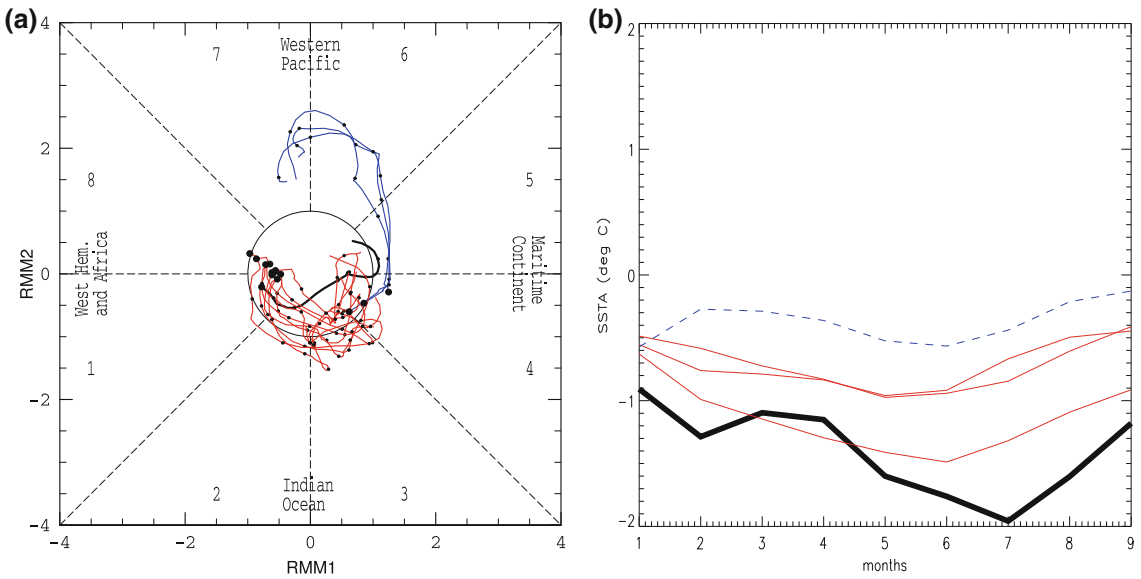

Fig. 13 July 1999 case study. **a** Phase diagram (Wheeler and Hendon 2004) of MJO propagation for a forecast start date of 19990701 for observed (ERA-40, *black line*), the ten ensemble members of POAMA-ALI (*red lines*) and the three ensemble members of POAMA-AMIP (*blue lines*). 30-day length trajectories are plotted, with the start date position marked by a *large dot* and *small dots* indicating 5-day intervals. **b** Niño3.4 SSTA over the 9 month forecast period, starting 19990701, for observed (Reynolds OI.v2 SST; *thick black line*), the POAMA-AMIP ensemble mean (*blue dashed line*) and the POAMA-ALI ensemble mean (*red lines* are three independent ensemble means each comprising three members taken from the original ten member ensemble)

shock resulting from the direct use of analyses as initial conditions could be detrimental to the forecast skill. There are a number of advantages of ALI. Namely, ALI:

- introduces more realistic atmosphere and land initial conditions into the hindcasts. Hindcasts will now better capture true intra-seasonal atmospheric states.
- allows greater consistency between the hindcasts (which are typically initialized from atmospheric historical reanalyses) and real-time forecasts (which are typically initialized from the most up to date atmospheric analyses), thus allowing better use of the hindcasts to assess intra-seasonal and seasonal forecast skill, and a more consistent bias correction.
- reduces the initialization shock compared to using ERA-40 atmospheric analyses directly as atmospheric initial conditions for the hindcasts.
- reduces the sensitivity to changes in the NWP forecast system from which real-time initial conditions are typically derived (i.e. ALI acts as a buffer to changes in the model).

The use of ALI as compared to AMIP initial conditions for forecasting El Niño and other tropical SST anomalies that are associated with coupled variability, results in improved skill at both seasonal and intra-seasonal time scales. These improvements in skill and thus the impact of the initial conditions vary a great deal as a function of forecast start month, lead time and region of analysis. The use of ALI results in an improvement in the SST anomaly correlation skill and lower MSE in the Niño3 and Niño3.4 regions out to at least 6 months lead time. Most of this improvement occurs in the June to November forecast start months. The reason for this is still unclear, but may be related to the typical ENSO life cycle. Our analysis suggests that the advances in forecast skill over the equatorial Pacific are due to improved initial anomalies that more realistically depict observed variability, rather than from an improved initial mean state, since the forecast drift in the POAMA-ALI experiment is actually slightly larger than that in POAMA-AMIP.

We have shown through two case studies how differences in atmospheric initial conditions between POAMA-ALI and POAMA-AMIP can translate into SST differences on the seasonal timescale via a coupled-response mechanism that, in these cases, includes the excitation of oceanic Kelvin waves that cause low frequency changes in SST anomalies in the eastern Pacific. Our results highlight that since we are dealing with a coupled system, initial errors (or differences between experiments) are amplified though a coupled process which can then lead to long lasting errors (or differences). In these cases, more realistic atmospheric initialization improved the prediction of ENSO over the 9 month forecasts, although the overall predictability of the events was probably still dominated by the ocean initial state.

Apart from the important increases in the skill of the seasonal forecast system, ALI has allowed POAMA to be an intra-seasonal to interannual forecast system, bridging the gap between weather and climate forecasting. The real-

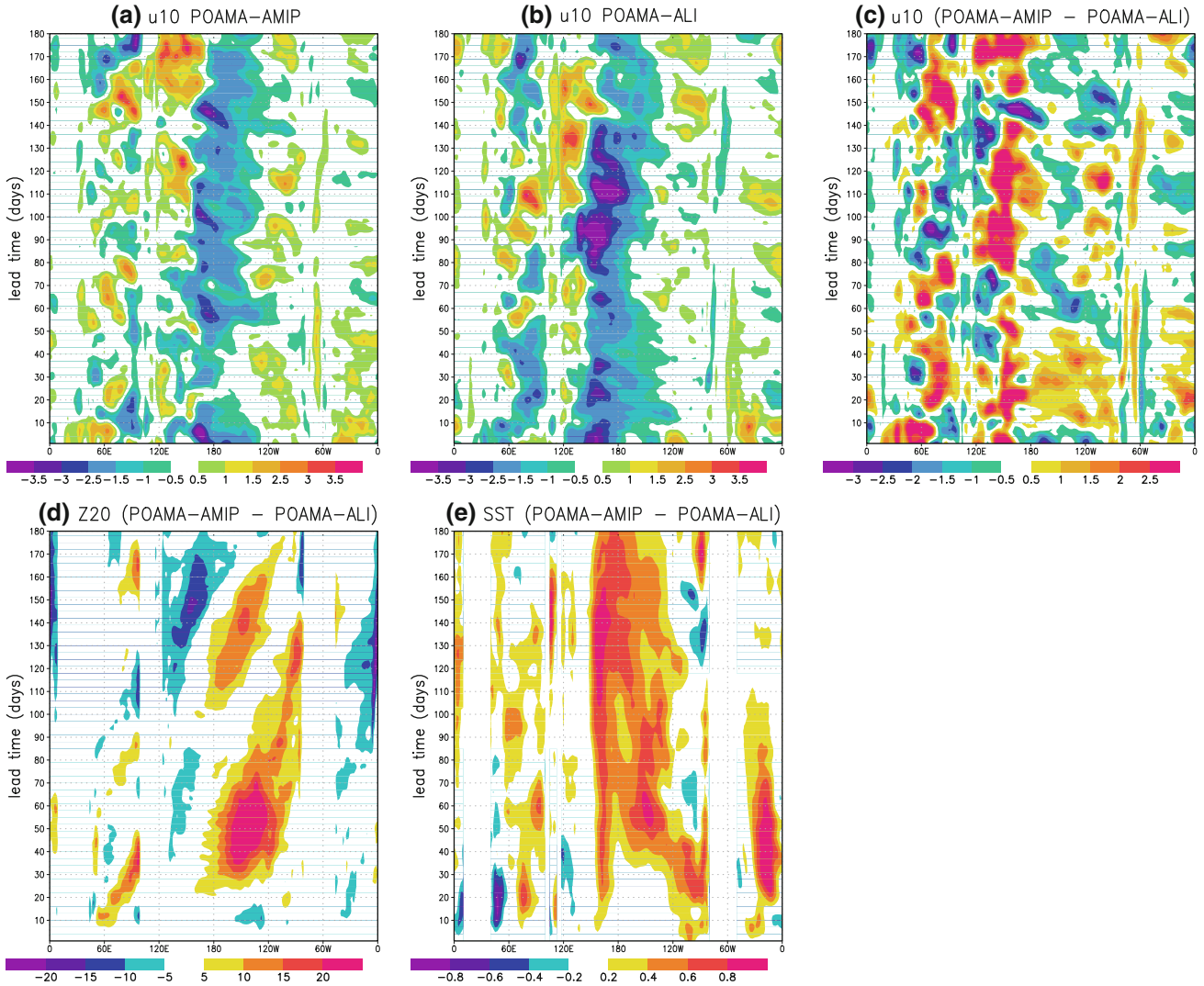

Fig. 14 Longitude-lead time plots for forecasts starting on 1 July 1999 of **a** POAMA-AMIP u10 (m s^{-1}) anomalies averaged between 5°S and 5°N (contour interval 0.5 m s^{-1}), **b** POAMA-ALI u10 (m s^{-1}) anomalies, and POAMA-AMIP minus POAMA-ALI anomalies for **c** u10 (m s^{-1}) (contour interval 0.5 m s^{-1}), **d** depth of the 20°C isotherm (m) along the equator (Z20) (contour interval 5 m) and **e** SST (°C) averaged between 5°S and 5°N (contour interval 0.2°C)

time POAMA system has always been initialised with real-atmospheric states and so could be used to predict MJO and intra-seasonal activity. However, the intra-seasonal hindcast skill of POAMA-1 was not assessed because the hindcasts were initialized with AMIP-type initial conditions that contain no real information about intraseasonal variability. In addition, because the hindcast dataset of POAMA-1 was inconsistent with the real-time system, the real-time intra-seasonal forecasts could not be adequately calibrated using the hindcast dataset. Our future challenge with the POAMA system in terms of initialisation is to implement coupled ALI–ocean initialisation. An improved balance between the atmosphere and SST initial conditions may help to reduce the shock of initialisation and coupled model biases.

Acknowledgments This research was funded in part by the South Eastern Australian Climate Initiative (SEACI). Andrew Marshall, Eun-Pa Lim, David Anderson and 2 anonymous reviewers are thanked for their useful comments in the preparation of this manuscript.

References

Alves O, Wang G, Zhong A, Smith N, Tzeitkin F, Warren G, Shiller A, Godfrey S, Meyers G (2003) POAMA: Bureau of Meteorology operational coupled model forecast system. National Drought Forum, 15/16 April, Brisbane

Anderson JL, Ploshay JJ (2000) Impact of initial conditions on seasonal simulations with an atmospheric general circulation model. Q J R Meteorol Soc 126:2241–2264

Balmaseda, M Anderson D (2009) Impact of initialization strategies and observations on seasonal forecast skill. Geophys Res Lett. doi:10.1029/2008GL035561

Bergman JW, Hendon HH, Weikman KM (2001) Intraseasonal air–sea interactions at the onset of El Niño. J Clim 14:1702–1719

Boulanger J-P, Durand E, Duvel J-P, Menkes C, Delecluse P, Imbard M, Lengaigne M, Madec G, Masson S (2001) Role of non-linear oceanic processes in the response to westerly wind events: new implications for the 1997 El Niño onset. Geophys Res Lett 28:1603–1606

Burgers G, Balmaseda MA, Vossepoel FC, Oldenborgh G, Leeuwen P (2002) Balanced ocean data assimilation near the Equator. J Phys Oceanogr 32:2509–2519

Chen D, Cane MA, Kaplan A, Zebiak SE, Huang D (2004) Predictability of El Nino over the past 148 years. Nature 428: 733–736

Colman R, Deschamps L, Naughton M, Rikus L, Sulaiman A, Puri K, Roff G, Sun Z, Embury G (2005) BMRC atmospheric model (BAM) version 3.0: comparison with mean climatology. BMRC research report no. 108. Bureau of Meteorology, Melbourne

Galanti E, Tziperman E, Harrison M, Rosati A, Sirkes Z (2003) A study of ENSO prediction using a hybrid coupled model and the adjoint method for data assimilation. Monthly Weather Rev 131:2748–2764

Hendon HH, Wheeler MC, Zhang C (2007) Seasonal dependence of the MJO–ENSO relationship. J Clim 20:531–543

Ji M, Behringer DW, Leetmaa A (1998) An improved coupled model for ENSO prediction and implications for ocean initialization. Part II: The coupled model. Monthly Weather Rev 126:1022–1034

Kanamitsu M, Kumar A, Juang H-MH, Schemm JK, Wang W, Yang F, Hong S-Y, Peng P, Chen W, Moorthi S, Ji M (2002) NCEP dynamical seasonal forecast system 2000. Bull Am Meterol Soc 83:1019–1037

Keenlyside N, Latif M, Botzet M, Jungclaus J, Schulzweida U (2005) A coupled method for initializing El Niño Southern Oscillation forecasts using sea surface temperature. Tellus 57A:340–356

Kessler WS, Kleeman R (2000) Rectification of the Madden–Julian oscillation into the ENSO cycle. J Clim 13:3560–3575

Kirtman B (2006) Initialization strategies for climate forecast system. Sci Technol Infus Clim Bull (NOAA), January 2006

Lengaigne M, Boulanger J-P, Menkes C, Madec G, Delecluse P, Guilyardi E, Slingo J (2003) The March 1997 Westerly wind event and the onset of the 1997/98 El Niño: understanding the role of the atmospheric response. J Clim 16:3330–3343

Lim E-P, Hendon HH, Hudson D, Wang G, Alves O (2009) Dynamical forecast of inter El-Nino variations of tropical SST and Australian spring rainfall. Monthly Weather Rev 137:3796–3810

Luo J, Masson S, Behera S, Shingu S, Yamagata T (2005a) Seasonal climate predictability in a coupled OAGCM using a different approach for ensemble forecasts. J Clim 18:4474–4497

Luo J, Masson S, Roeckner E, Madec G, Yamagata T (2005b) Reducing climatology bias in an ocean–atmosphere CGCM with improved coupling physics. J Clim 18:2344–2360

Manabe S, Holloway J (1975) The seasonal variation of the hydrological cycle as simulated by a global model of the atmosphere. J Geophys Res 80:1617–1649

Marshall AG, Alves O, Hendon HH (2008) An enhanced moisture convergence-evaporation feedback mechanism for MJO air–sea interaction. J Atmos Sci 65:970–986

McPhaden MJ (1999) Genesis and evolution of the 1997–98 El Niño. Science 283:950–954

Phelps MW, Kumar A, O'Brien JJ (2004) Potential predictability in the NCEP CPC dynamical seasonal forecast system. J Clim 17:3775–3785

Phillips TJ, Potter GL, Williamson DL, Cederwall RT, Boyle JS, Fiorino M, Hnilo JJ, Olson JG, Xie S, Yio JJ (2004) Evaluating parameterizations in general circulation models: climate simulation meets weather prediction. Bull Am Meterol Soc 85:1903–1915

Rashid H, Hendon HH, Alves O, Wheeler M (2010) Predictability of the Madden–Julian oscillation in the POAMA dynamical seasonal prediction system. Clim Dyn. doi:10.1007/s00382-010-0754-x

Rayner NA, Parker DE, Horton EB, Folland CK, Alexander LV, Rowell DP, Kent EC, Kaplan A (2003) Global analyses of sea surface temperature, sea ice, and night marine air temperature since the late nineteenth century. J Geophys Res 108:4407. doi: 10.1029/2002JD002670

Reichler TJ, Roads JO (1999) The role of boundary and initial conditions for dynamical seasonal predictability. Nonlinear Proc Geophys 10:211–232

Reynolds R, Rayner NA, Smith TM, Stokes DC, Wang W (2002) An improved in situ and satellite SST analysis for climate. J Clim 15:1609–1625

Rienecker M (2003) Workshop report: coupled data assimilation workshop, Portland, April 21–23, 2003, sponsored by NOAA/OGP. Available at http://www.usclivar.org/Meeting_Files/SSC-11/CoupledDA_rept_final.pdf

Schiller A, Godfrey J, McIntosh P, Meyers G (1997) A global ocean general circulation model climate variability studies. CSIRO marine research report no. 227, CSIRO, Australia

Schiller A, Godfrey J, McIntosh P, Meyers G, Smith N, Alves O, Wang O, Fiedler R (2002) A new version of the Australian Community Ocean Model for seasonal climate prediction. CSIRO marine research report no. 240, CSIRO, Australia

Seaman R, Bourke W, Steinle P, Hart T, Embery G, Naughton M, Rikus L (1995) Evolution of the Bureau of Meteorology's global assimilation and prediction system. Part 1: Analysis and initialisation. Aust Meterol Mag 44:1–18

Shi L, Alves O, Hendon HH, Wang G, Anderson D (2009) The role of stochastic forcing in ensemble forecasts of the 1997/98 El Nino. J Clim 22:2526–2540

Smith NR, Blomley JE, Meyers G (1991) A univariate statistical interpolation scheme for subsurface thermal analyses in the tropical oceans. Prog Oceanogr 28:219–256

Stockdale TN (1997) Coupled ocean–atmosphere forecasts in the presence of climate drift. Monthly Weather Rev 125:809–818

Stockdale TN, Anderson DLT, Alves JOS, Balmaseda MA (1998) Global seasonal rainfall forecasts using a coupled ocean–atmosphere model. Nature 392:370–373

Uppala SM, Kallberg PW, Simmons AJ et al (2005) The ERA-40 re-analysis. Q J R Meteorol Soc 131:2961–3012

Valcke S, Terray L, Piacentini A (2000) Oasis 2.4, Ocean atmosphere sea ice soil: user's guide. TR/CMGC/00/10, CERFACS, Toulouse, France

van Oldenborgh GJ (2000) What caused the onset of the 1997–98 El Niño? Monthly Weather Rev 128:2601–2607

Vitart F, Balmaseda M, Ferranti L, Anderson D (2003) Westerly wind events and the 1997/98 El Niño event in the ECMWF seasonal forecasting system: a case study. J Clim 16:3153–3170

Wang G, Alves O, Smith N (2005) BAM3.0 tropical surface flux simulation and its impact on SST drift in a coupled model. BMRC research report no. 107, Bureau of Meteorology, Melbourne

Wang B, Lee J-Y, Kang I-S et al (2009) Advance and prospectus of seasonal prediction: assessment of the APCC/CliPAS 14-model ensemble retrospective seasonal prediction (1980–2004). Clim Dyn 33:93–117

Wheeler MC, Hendon HH (2004) An all-season real-time multivariate MJO index: development of an index for monitoring and prediction. Monthly Weather Rev 132:1917–1932

Zhang C, Hendon HH, Kessler WS, Rosati AJ (2001) Meeting summary: a workshop on the MJO and ENSO. Bull Am Meteor Soc 82:971–976

Zhang R-H, Zebiak SE, Kleeman R, Keenlyside N (2003) A new intermediate coupled model for El Niño simulation and prediction. Geophys Res Lett 30:2012

Zhang C, Dong M, Gualdi S, Hendon H, Maloney E, Marshall A, Sperber K, Wang W (2006) Simulations of the Madden–Julian oscillation in four pairs of coupled and uncoupled global models. Clim Dyn 27:573–592

Zhong A, Alves O, Hendon H, Rikus L (2006) On aspects of the mean climatology and tropical interannual variability in the BMRC atmospheric model (BAM 3.0). BMRC research report no. 121, Bureau of Meteorology, Melbourne